Chem. Anal. (Warsaw), **54**, 1219 (2009)

Evaluation of Various Types of Micronebulizers and Spray Chamber Configurations for Microsamples Analysis by Microwave Induced Plasma Optical Emission Spectrometry

by H. Matusiewicz[1]*, M. Ślachciński[1], B. Almagro[2] and A. Canals[2]

[1] *Politechnika Poznańska, Department of Analytical Chemistry, 60-965 Poznań, Poland*
[2] *Departamento de Quimica Analitica, Nutrición y Bromatologia, Universidad de Alicante, Apdo. 99, E-03080 Alicante, Spain*

Keywords: Microwave induced plasma; Optical emission spectrometry; Reference materials; Nebulizers; Microsamples

A new and more efficient atomization principle (*i.e.* Flow Blurring) was introduced to the microwave-induced plasma optical emission spectrometric (MIP–OES) analysis. Analytical behaviors of a nebulizer based on the Flow Blurring technology (*i.e.* Flow Blurring nebulizer, FBN) and of five different microliter-nebulizers: a High Efficiency Nebulizer (HEN), a Demountable Direct Injection High Efficiency Nebulizer (D–DIHEN), an AriMist (AM), a MiraMist CE (MMCE), and an ultrasonic nebulizer (NOVA–1) were compared to the behavior of a conventional Meinhard pneumatic concentric nebulizer (PN) for elemental analysis of liquid microsamples, working at low liquid flow rates and applying the argon-helium MIP–OES method. Analytical performance of the nebulization systems were characterized by limits of detection (LODs) and precision (RSDs), which were determined experimentally. Atomic emission was measured for Ba, Ca, Cd, Cu, Fe, Mg, Mn, Pb and Sr. The analysis of certified reference materials (TORT–1, Human Hair No. 13, Lichen IAEA–336, Soya Bean Flour INCT–SBF–4) was performed to determine accuracy and precision available with the investigated nebulization systems. Certified materials were microwave/nitric acid-digested and analyzed by external calibration. In general, the results indicated that both FBN and D–DIHEN nebulizers gave rise to higher emission signals and slightly lower LOD values than other nebulizers.

* Corresponding author. E-mail: Henryk.Matusiewicz@put.poznan.pl

Zbadano efektywność tworzenia aerozolu i jego transportu do plazmy mikrofalowej przez sześć mikrorozpylaczy: HEN (ang. *High Efficiency Nebulizer*), D–DIHEN (ang. *Demountable Direct Injection High Efficiency Nebulizer*), AM (AriMist), MMCE (MiraMist CE), FBN (ang. *Flow Blurring Nebulizer*) oraz rozpylacz ultradźwiękowy NOVA–1 w porównaniu z klasycznym rozpylaczem koncentrycznym (PN). Rozpylacze, z wyjątkiem wyposażonego we własną komorę NOVA–1, połączono z kwarcową minikomorą cyklonową "Electron" z płaszczem chłodzącym. Zbadano jakość aerozolu pierwszorzędowego i trzeciorzędowego tworzonego przez badane rozpylacze/komorę mgielną na podstawie rozkładu średnic i prędkości kropli oraz efektywności transportu rozpuszczalnika i składnika oznaczanego (Mg). Do oceny przydatności badanych mikrorozpylaczy do oznaczania Ba, Ca, Cd, Cu, Fe, Mg, Mn, Pb i Sr w różnych próbkach zastosowano biologiczne i środowiskowe certyfikowane materiały odniesienia: TORT–1, Human Hair No. 13, Lichen IAEA–336, Soya Bean Flour INCT–SBF–4. Oznaczenia wykonano techniką krzywej wzorcowej za pomocą spektrometru emisyjnego Plasmaquant 100 (Carl Zeiss, Niemcy). Granicę wykrywalności obliczono zgodnie z zaleceniami IUPAC, z trzykrotnej wartości odchylenia standardowego ślepej próby (3σ) na podstawie powierzchni uzyskanych sygnałów analitycznych.

Although liquid sample introduction by the means of pneumatic nebulization is the most common in inductively coupled plasma (ICP) and microwave induced plasma (MIP) spectrometries, both methods suffer from the inefficient use of a sample and thus have the same limitations. The main disadvantages of the most of pneumatic nebulizers are their low efficiency (< 5%), high sample consumption, and wide size distribution of aerosol droplets. In order to increase the efficiency of sample introduction and to reduce the consumption rate, micronebulizers operating in the microliter sample flow rate range have been developed [1, 2].

The development of pneumatic micronebulizers coupled to spray chambers dedicated to work at very low liquid flow rates (*i.e.* of the order of several tens of microliters per minute) has opened the possibility of easily analyzing the samples by atomic spectrometry when the amount of a sample is limited (lower than 1 mL). Such a situation is encountered in many areas – forensic, biological, clinical, geological, semiconductor, on-chip technology, *etc*.). These advances also allow for efficient coupling of separation techniques, such as capillary electrophoresis, nanoliquid chromatoghraphy, and plasma atomic spectrometry (ICP, MIP, DCP).

Application of nebulizers to the sample introduction into the microwave–induced plasma sources has become possible since MIPs could be operated at the atmospheric pressure [3]. This system allowed liquid aerosols to be nebulized directly into the atmospheric discharge. Microwave plasmas are normally operated at substantially lower applied power than inductively coupled plasma (ICP) devices. Low power levels do not produce sufficiently energetic plasma for efficient processes in the plasma (desolvation, volatilization, *etc.*). In addition, stability of plasma can be seriously affected when solutions are injected directly. For these reasons, microflow devices are ideal for this excitation source.

In order to handle low liquid sample volumes, the system should be operated at low flow rates of the order of several microliters per min. Under these conditions nebulizer must exhibit a good performance, such as good figures of merit and low dead volumes. Over the past several years, some nebulizer – spray chamber coupled systems for microwave–induced plasma optical emission spectrometry (MIP–OES) have been developed in order to reduce both the consumption of the liquid by sample introduction systems and the amount of waste. Among these systems are: glass frit nebulizer [4, 5], thermospray nebulizer [6], ultrasonic nebulizer [7], Hildebrand grid nebulizer [8], glass capillary array nebulizer [5, 9] and V-groove Babington nebulizer [10, 11]. It is typical for micro-nebulizers that they are commercially available in the form of low-volume (< 20 mL) spray chambers. Although each nebulizer and spray chamber combination has its own characteristics and properties, determining which combination and design are best suited for a specific application is paramount in obtaining reproducible and superior figures of merit.

Although great efforts have been made to supply a nebulizer for each specific application (*i.e.* sample viscosity, salt and solids contents), no universal nebulizer applicable for all sample types exists. Having this in mind, a new hydrodynamic principle for spectrochemical analysis (*i.e.*, Flow Focusing) has been introduced by Canals *et al.* [12–14]. Recently, a systematic comparison between a flow-focusing nebulizer (FFN) and two micronebulizers (*i.e.*, micro3 (M3) and microcapillary array nebulizer (NAR–1)) for elemental analysis of liquid samples by MIP–OES has been performed; the best analytical performance was observed for FFN [15].

In 2005 A.M. Ga án-Calvo [16] introduced a novel hydrodynamic principle (*i.e.* Flow Blurring) that might be useful for liquid sample introduction into atomic spectrometers. After a geometrical modification on FFN, a new and more efficient atomization principle emerged. A description of this new hydrodynamic principle is available in reference [16] and a detailed description of analytical implications on ICP–OES of this atomization principle is presented shortly in reference [17]. Figure 1 shows a comparison between the Flow Focusing and Flow Blurring atomization principles.

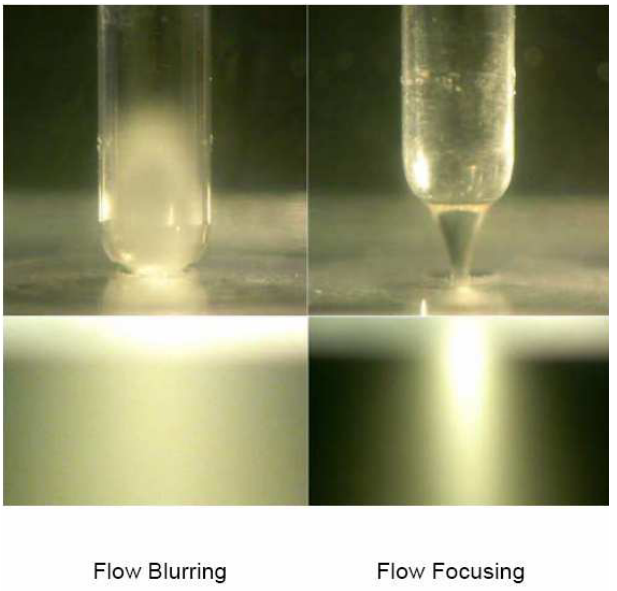

Figure 1. Flow focusing *vs* flow blurring (from A.M. Ga án-Calvo, with permission)

This work had two main goals: (i) to evaluate the Flow Blurring technology for liquid sample introduction into MIP–OES, and (ii) to compare the analytical behavior of a nebulizer based on the Flow Blurring technology with some popular and commercial micronebulizers used in MIP–OES. Our assessment was based on the main figures of merit (*i.e.*, sensitivity, signal stability, limits of detection, *etc.*) estimated for aqueous sample solutions; a commercially available pneumatic concentric nebulizer was used as a reference. Four different certified reference materials were analyzed against aqueous standards so as to assess the effect of possible interferences on the results. Analytical potentialities were also discussed.

EXPERIMENTAL

MIP-OES instrumentation and operating conditions

A Carl Zeiss Echelle spectrometer (Model PLASMAQUANT 100) with fiber-optical light-guides and photomultiplier tubes (PMT) and TE_{101} microwave plasma cavity assembly was used; it was essentially the same as the one described previously [18, 19]. Instrumental settings and operational parameters of the experimental MIP–OES system are summarized in Table 1. A schematic diagram of the entire experimental setup (*i.e.* sample introduction system-MIP–OES) is shown in Figure 2.

Table 1. Instrumental parameters of the Echelle spectrometer Ar/He–MIP–OES system

Mounting	Czerny-Turner in tetrahedral set-up
Focal length, mm	500
Spectral range, nm	193–852
Order lines	28^{th}–123rd
Microwave frequency, MHz	2450
Microwave power, W	100–200, variable
Microwave cavity	TE_{101} rectangular, water cooled
Microwave generator	700 W, MPC–01 (Plazmatronika Ltd., Wrocław, Poland)
Plasma viewing mode	Axial
Plasma torch, axial position	Quartz tube, 3.0 mm I.D., air cooled
Argon flow rate, mL min^{-1}	400–1500, variable
Plasma supporting argon/helium flow rate, mL min^{-1}	80–300, variable
Sample uptake rate, µL min^{-1}	4–2500
Read	On-peak
Integration time, s	0.1
Background correction	Fixed point
Determination	Simultaneous
Wavelength, nm (line type)	Ba 455.403 (II), Ca 317.933 (II) Ca 393.366 (II), Cd 226.502 (II) Cu 324.754 (I), Fe 238.204 (II), Mg 279.553 (II), Mg 285.213 (I), Mn 257.611 (II), Pb 405.783 (I), Sr 407.771 (II), Zn 213.857 (I)

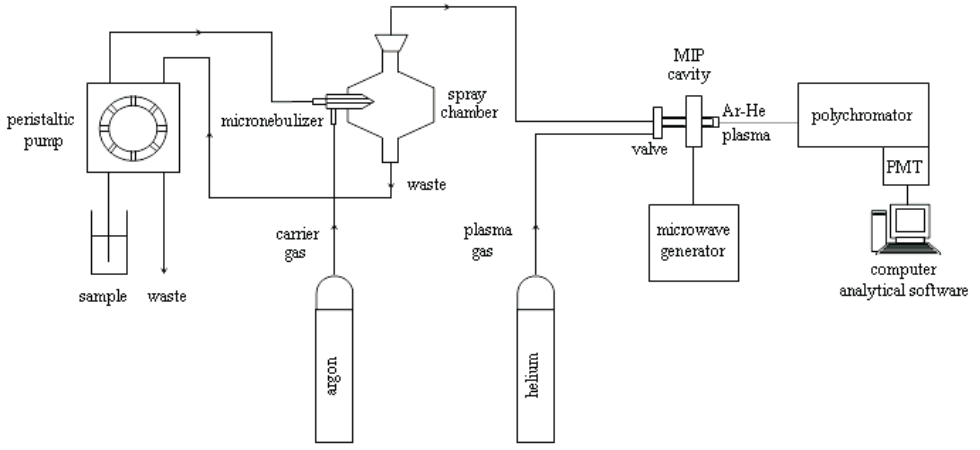

Figure 2. A diagram of the elaborated micronebulizer–MIP–OES system

Sample introduction systems

Five different micronebulizers: a High Efficiency Nebulizer (HEN) (Meinhard Glass Products, Golden Colorado, USA), a Demountable Direct Injection High Efficiency Nebulizer (D–DIHEN) (Analab, Strasbourg, France), an Ari Mist (AM) and a MiraMist CE (MMCE) (Burgener Research Inc., Mississauga, Canada), a Flow Blurring nebulizer (FBN) (Ingeniatrics Tecnologias, Sevilla, Spain), and three spray chambers: a 'Cinnabar' cyclonic spray chamber (Glass Expansion, West Melbourne, Australia), an 'Electron' mini-cyclonic jacketed spray chamber for low uptakes (EPOND, Vevey Switzerland) and a Quasi-Direct Injection system for very low uptakes (QuDIN) (EPOND, Vevey Switzerland) were tested. A TR–30–A3 (PN) commercial pneumatic concentric nebulizer (Meinhard Glass Products, Golden, Colorado, USA) was used as a reference in comparison studies, since it is the standard nebulizer in many plasma-based instruments. Apart from the pneumatic micro-nebulizers mentioned above, an ultrasonic nebulizer (NOVA–1) without desolvation system based on a fundamentally different principle was proposed. In order to compare the behaviors of the tested nebulizers, an "Electron" (EPOND) quartz cyclonic spray chamber (*ca* 15 mL inner volume) was used as the reference system in combination with AM, D–DIHEN, FBN, HEN, MMCE and PN nebulizers to transport an aerosol towards the microwave plasma torch. NOVA–1, however, due to its special design and dimensions, was used with a different glass spray chamber (10 mL inner volume).

Liquid samples were introduced *via* nebulizers using a Gilson Minipuls 3 peristaltic pump (Villiers Le Bel, France). A gas flow rate was controlled by a mass flow controller (DHN, Warsaw, Poland) with a pressure regulator. Argon was used as a nebulizing-carrier gas and plasma gas; helium was used as a plasma gas.

Aerosol characterization and transport variables

Drop size and velocity distributions of primary and tertiary aerosols were determined using a two-dimensional Phase Doppler Particle Analyzer (2D–PDPA, TSI Inc., USA) [15, 20, 21]. Primary aerosol was sampled at a distance of 5.0 mm from the nebulizer tip along the centerline of the aerosol. Tertiary aerosol was measured at a distance of 1.0 mm from the end of spray chambers, and at the centerline of the chambers' exits. To follow the conditions in MIP, the nebulizers were horizontally positioned for primary aerosol diameter-

velocity measurements, whereas tertiary aerosol was sampled vertically. In each PDPA acquisition, approximately 10 000 droplets were measured to determinate particle size and velocity distributions.

Analyte and solvent transport rates were measured by the means of direct collection methods [22, 23]. Solvent transport rates were measured at the outlet of spray chambers. Tertiary aerosol was being collected for 5–30 min using a U-tube packed with a silica gel; S_{tot} was evaluated by weighing the tube before and after its exposition to the aerosol. For the total analyte transport rates, a 500 mg L^{-1} manganese standard solution (Merck, Darmstadt, Germany) was nebulized for 5–45 min and tertiary aerosol was collected on glass fibre filters (Type GF/C, 47 mm diameter, 1.2 μm pore size; Whatman, Maidstone, England). The analyte was extracted with 1 mol L^{-1} nitric acid (Merck, Darmstadt, Germany) for 20 min at 80°C. Finally, the solutions were diluted with distilled water and analyzed by flame atomic absorption spectrometry (SpectrAA 10 Plus, Varian, Australia). Each measurement was performed in triplicate.

Gases and reagents

Compressed pure argon and helium gases (N–50 purity, 99.999%) obtained from BOC GAZY (Poznań, Poland) were used as plasma gases.

Standard solutions were prepared from a 1000 mg L^{-1} stock solution (ICP Multi-element Standard Solution IV CertiPURs, Merck, Darmstadt, Germany). Working standard solutions were freshly prepared daily by diluting the appropriate aliquots of the stock solution in 1 mol L^{-1} HNO_3 prepared from 69% high purity acid (Merck) and pure water.

HNO_3 (69%, v/v, trace pure, Merck, Germany) of the highest quality grade was used. 30% (v/v) H_2O_2 solution was obtained from POCh (Gliwice, Poland).

Water was initially deionized (Model DEMIWA 5 ROSA, Watek, Czech Republic) and then doubly distilled in a quartz apparatus (Heraeus Bi18, Hanau, Germany).

Reference materials

Applicability of the method described in this work was assessed using four reference materials: TORT–1 (Lobster hepatopancreas) supplied by the National Research Council of Canada (NRCC, Ottawa, Canada), Human Hair No. 13 from the National Institute for Environmental Studies (NIES, Japan), Lichen IAEA-336 from the International Atomic Energy Agency (Vienna, Austria) and Soya Bean Flour INCT–SBF–4 supplied by the Institute of Nuclear Chemistry and Technology (Warsaw, Poland).

Microwave digestion system

A laboratory-made prototype of a high pressure temperature-focused microwave heating digestion system, equipped with a closed TFM–PTFM vessel, based on a design outlined in detail by Matusiewicz [24], was employed for wet-pressure sample digestion.

ANALYTICAL PROCEDURES

Microwave-assisted sample digestion at high pressure in PTFE vessels

The applied microwave-assisted digestion method has been described in a previous work [15].

Simplex optimization procedure

A simplex optimization approach was undertaken to establish the best conditions for liquid nebulization, transport, and excitation. The optimized parameters along with the ranges over which optimization experiments were conducted are listed in Table 2.

Table 2. Optimum operating conditions for the determination of elements in soluble materials by MIP–OES using microliquid nebulization systems

Parameter	Nebulizer						
	PN	AM	MMCE	FBN	HEN	D–DIHEN	NOVA–1
Applied power, W	180	160	160	170	150	160	160
Nebulizer pressure, bar	5.6	5	5.2	5	9	2.5	4
Argon gas flow rate, mL min^{-1}	1100	600	800	600	600	150	400
Helium gas flow rate, mL min^{-1}	150	250	200	250	200	200	150
Sample liquid uptake rate (pumped), μL min^{-1}	1 500	50	8	90	100	25	10

Simplex optimization experiments were performed using a Multisimplex AB (Karlskrona, Sweden) software package. Optimization was carried out for each nebulizer in order to establish "real" experimental conditions. In all experiments the "electron" spray chamber was used. Net value of the signal-to-background ratio (S/B) was taken as the criterion of merit. Some preliminary univariate experiments (screening) were performed prior to the simplex optimization in order to establish the boundary values for each parameter. Three measurements for each variable were conducted at the value of interest. Between each two consecutive experiments, a blank corrective experiment was run to ensure stable and repeatable results.

The optimum conditions established in this procedure were then applied to the standard element solutions in order to quantify the elements present in the dissolved samples.

MIP–OES analysis

MIP–OES analyses were done as described in ref. [15], following the instrumental and operational conditions listed in Tables 1 and 2.

RESULTS AND DISCUSSION

Optimization of operating parameters

First, the performance of seven nebulizers was compared using aqueous solutions. To this end, the characteristics of the aerosols, the amount of solution transported, and analytical figures of merit in MIP–OES were evaluated. Finally, practical

application of the determination of selected elements in reference materials was presented.

Optimization of the wavelength used for determination was not carried out because it was pre-selected by the producer of the polychromator.

Preliminary analytical performance of Ar/He–MIP was examined by measuring the S/B ratio for selected elements. However, detailed optimization of the parameters of gases for the analytes was not undertaken, as the values corresponding to the excitation and ionization conditions for MIP–OES with pneumatic nebulization were readily available from the literature ([25] and references cited therein). The comparison of these parameters obtained for the mixed plasma with those for pure argon plasma and helium plasma with pneumatic nebulization showed that the detection limits achieved with the mixed plasma were better than those obtained with the pure plasma. In addition, the Ar + 20% He MIP mixture exhibited higher tolerance to water loading. Taking into account the above effects, Ar/He–MIP was selected for all the subsequent experiments, for a plasma gas composition of *ca* 80% Ar and 20% He; this is in agreement with the earlier results [25].

Simplex optimization of operational variables

Two different types of experimental variables affected the studied method. These were: variables controlling the emission response in the microwave plasma, *i.e.* microwave forward power of the microwave generator, and variables such as Ar carrier flow rate and sample uptake rate that regulated the sample transport. Followed by the univariate search for the optimum magnitude of the applied power, nebulizing-carrier gas flow rate, and sample uptake rate, a multivariate simplex optimization was performed to establish the optimum experimental parameters for low detection limits of selected elements. For each nebulizer the optimization was completed in 16 steps, which took approximately 2 h. These values were chosen following the recommendations given in the literature and preliminary experiments with solution nebulization by the MIP–OES method. The effectiveness of the simplex procedure was confirmed with univariate search, which helped to verify that the optimum lay near the simplex value. The optimized parameters are listed in Table 2.

Microwave forward power

MIP is normally operated at a low power from the range 50–150 W. In this work, stable Ar/He plasma could be maintained at the forward power level higher than 100 W. Between 100 and 200 W, neither the intensities of spectral lines nor the S/B ratios depended on the power magnitude in a way indicating the pronounced optimum. In addition, the stability of the background and line signals did not vary significantly with the power magnitude in the stated range. In general, for all analytical

lines of the studied elements, S/B ratios usually tended to level off when the microwave power approached 180, 160, 160, 170, 150, 160 and 160 W for PN, AM, MMCE, FBN, HEN, D–DIHEN and NOVA–1, respectively. The intensities of the spectral lines also leveled off, but more slowly. Taking into account the above effects, the optimized power of 150–70 W was selected as acceptable for a practical working range.

Carrier argon and plasma helium/argon flow rates

The effect of plasma (support) helium gas flow rate was optimized and selected based upon our previous experience and maintaining plasma stability and shape. Stable operation of the plasma was obtained at the gas flow rates of 150, 250, 200, 250, 200, 200 and 150 mL min^{-1} for PN, AM, MMCE, FBN, HEN, D–DIHEN and NOVA–1, respectively.

It was also observed that the flow rate of the carrier Ar gas stream had more significant influence on the emission intensities than the plasma support gas flow rate. The carrier Ar gas affected the formation of the plasma channel (annular configuration) [26], the residence time of the analyte in the plasma, and the aerosol generation and transport efficiency [12, 27]. To optimize the carrier (nebulizing) Ar gas flow for multi-element determination, the optimum flow for all elements was estimated in the total range of 50–1500 mL min^{-1} for all seven nebulizers. It was observed that the flow rate of the carrier Ar gas stream had a significant influence on the emission intensities and thus it was proved to be a critical parameter. In general, it was observed that when the flow rate ranged between (500–1500 mL min^{-1}) (400–1000 mL min^{-1}), (500–1100 mL min^{-1}), (400–1000 mL min^{-1}), (300–1000 mL min^{-1}), (50–200 mL min^{-1}) and (200–1000 mL min^{-1}) for PN, AM, MMCE, FBN, HEN, D–DIHEN and NOVA–1 nebulizers, respectively, the emission intensities reached maximum at 1100, 600, 800, 600, 600, 150 and 400 mL min^{-1} for PN, AM, MMCE, FBN, HEN, D–DIHEN and NOVA–1, respectively. When the flow rate was further increased above these values, the emission intensities of all elements decreased. The maxima resulted from the opposite effects of the nebulizing gas flow on the aerosol characteristics and transport and the interaction of the aerosol with the plasma. Increasing the nebulizing gas flow rate commonly caused a shift of both primary and tertiary drop size distributions to the smaller values. This, in turn, led directly to the higher analyte and solvent transport rates. However, these two transport rates exerted opposite effects on the net signal intensity. In addition, the higher the nebulizing-carrier gas flow, the smaller the residence time of droplets in the plasma. Therefore, the overall effect was reflected in the form of a maximum behavior [12]. Therefore, in this study 1100, 600, 800, 600, 600, 150 and 400 mL min^{-1} carrier argon flow rates were selected for PN, AM, MMCE, FBN, HEN, D–DIHEN and NOVA–1 nebulizers, respectively.

Sample uptake rate

Sample uptake rate was also proved to be important. When the sample pumping rate was greater than approximately 1500, 50, 8, 90, 100, 25 and 10 μL min^{-1} for PN, AM, MMCE, FBN, HEN, D–DIHEN and NOVA–1, respectively, it was found that the signal intensities did not increase further and started to decrease. For pneumatic nebulization and the increasing liquid flow, the primary drop size distribution was shifted to larger drop sizes. Nevertheless, the absolute amount of the aerosol volume contained in a smaller drop was increased [12]. Therefore, the higher the liquid flow was, the higher the analyte and solvent transport rates became; this led finally to the maximum in the signal *vs*. liquid flow dependence. Therefore, the sample uptake rate of 1500, 50, 8, 90, 100, 25 and 10 μL min^{-1} for PN, AM, MMCE, FBN, HEN, D–DIHEN and NOVA–1 nebulizers, respectively, was selected.

Analytical figures of merit

Detection limits obtained on a simultaneous multi-element basis for various nebulizers employed were compared to the results obtained using PN. A comparison of detection limits obtained by conventional nebulization (PN) and micro-nebulization (AM, MMCE, FBN, HEN, D–DIHEN, NOVA–1) for the set of lines tested is shown in Table 3. Limits of detection (LOD) corresponding to the optimized operating conditions and calculated using the IUPAC recommendation (based on $3\sigma_{blank}$ criterion) for the raw unsmoothed data are summarized in Table 3.

Table 3. Limits of detection (LOD) for the tested elements and nebulizers

Element	Line wavelength, nm	PN		AM		MMCE		FBN	
		μg mL^{-1}	% RSD	μg mL^{-1}	% RSD	μg mL^{-1}	% RSD	μg mL^{-1}	% RSD
Ba	455.403 (II)	0.085	7	0.071	8	0.093	8	0.025	4
Ca	393.366 (II)	0.044	5	0.026	7	0.052	6	0.010	5
Cd	226.502 (II)	0.054	8	0.032	8	0.042	8	0.007	7
Cu	324.754 (I)	0.009	7	0.008	8	0.086	6	0.003	7
Fe	238.204 (II)	0.075	6	0.037	9	0.153	7	0.008	8
Mg	285.213 (I)	0.052	8	0.026	6	0.008	7	0.003	3

(Continuation on the next page)

Table 3. (Continuation)

Element	Line wavelength, nm	PN		AM		MMCE		FBN	
		µg mL^{-1}	% RSD	µg mL^{-1}	% RSD	µg mL^{-1}	% RSD	µg mL^{-1}	% RSD
Pb	405.783 (I)	0.063	8	0.035	7	0.075	7	0.004	4
Sr	407.771 (II)	0.020	5	0.019	6	0.097	6	0.005	4
Zn	213.857 (I)	0.075	7	0.015	8	0.020	5	0.010	6

Element	Line wavelength, nm	HEN		D–DIHEN		NOVA–1	
		µg mL^{-1}	% RSD	µg mL^{-1}	% RSD	µg mL^{-1}	% RSD
Ca	393.366 (II)	0.018	5	0.009	5	0.012	5
Cd	226.502 (II)	0.012	8	0.008	7	0.005	7
Cu	324.754 (I)	0.004	5	0.005	6	0.003	6
Fe	238.204 (II)	0.015	8	0.029	8	0.009	6
Mg	285.213 (I)	0.011	4	0.006	4	0.010	5
Mn	257.611 (II)	0.009	4	0.005	6	0.006	6
Pb	405.783 (I)	0.013	5	0.007	6	0.011	7
Sr	407.771 (II)	0.011	4	0.006	4	0.009	5
Zn	213.857 (I)	0.012	7	0.008	7	0.008	6

FBN provided lower limits of detection than other nebulizers for almost all the elements evaluated in the axially-viewed microwave plasma with a 1% nitric acid matrix.

Detection limits presented in Table 3 were calculated from the standard deviation (3σ) of six measurements of the known injection volume of the blank solution. The values of detection limit decrease in the order FBN ≤ D–DIHEN < NOVA–1 < HEN < AM < PN < MMCE.

Precision of replicate determinations was calculated from RSD (%) of the mean of six replicate measurements of the element standard using a mass 50-fold above the LOD. Precision of FBN was similar to or slightly better than that of other nebulizers.

Precision of determination of the elements ranged from 3 to 9% for original liquid samples (evaluated as peak height) and was probably largely affected by instability of the microwave plasma source. These values can be considered satisfactory, especially owing to the large number of parameters governing the performance of the analytical technique. They reflect the cumulative imprecision of sample nebulization, transfer of aerosols, excitation, and detection steps.

Drop size and velocity distributions of primary aerosols

Representative primary drop size and velocity distributions are presented in Figure 3(a) and Figure 4(a), respectively; they were obtained for all nebulizers under optimized conditions. The main role of spray chambers was to remove large and fast droplets (larger than the cut-off (d_c) diameter of the chamber) from the aerosol. Cut-off diameter was mainly a function of the experimental conditions and geometry of the spray chamber. Typically, this value ranges between 15 μm and 20 μm [13, 28]. The number percentage of primary aerosol contained in droplets having sizes smaller than 20 μm was 93%, 95% and 85% for AM, MMCE and PN, respectively and near 100 % for D–DIHEN, FBN and HEN (Fig. 3(a)). Droplet size distribution of the aerosols from D–DIHEN, FBN, and HEN was much finer (the fraction of small droplets was higher and more monodisperse) than that produced by other nebulizers. Mean velocities of primary aerosol were 39, 73, 36, 45, 25 and 31 m s^{-1} for AM, MMCE, FBN, HEN, D–DIHEN and PN, respectively. MMCE used the lowest Q_l and high Q_g, hence showed the highest velocity. DIHEN used low Q_g and an intermediate Q_l, hence showed the smallest velocity.

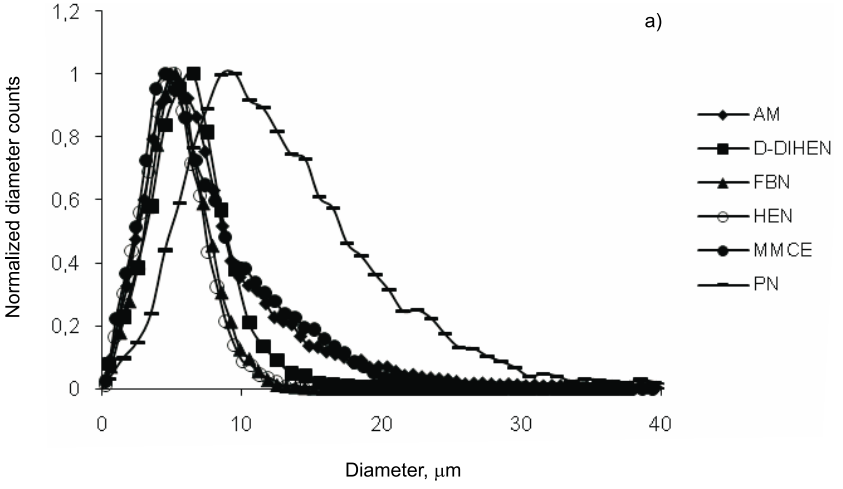

Figure 3. Droplet size distributions of primary (a) and tertiary (b)–(d) aerosols from different nebulizers and spray chambers. (Continuation on the next page)

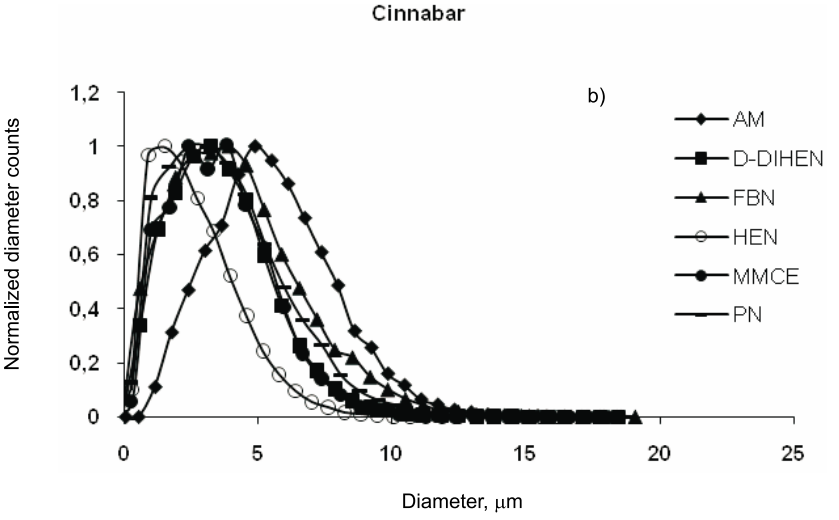

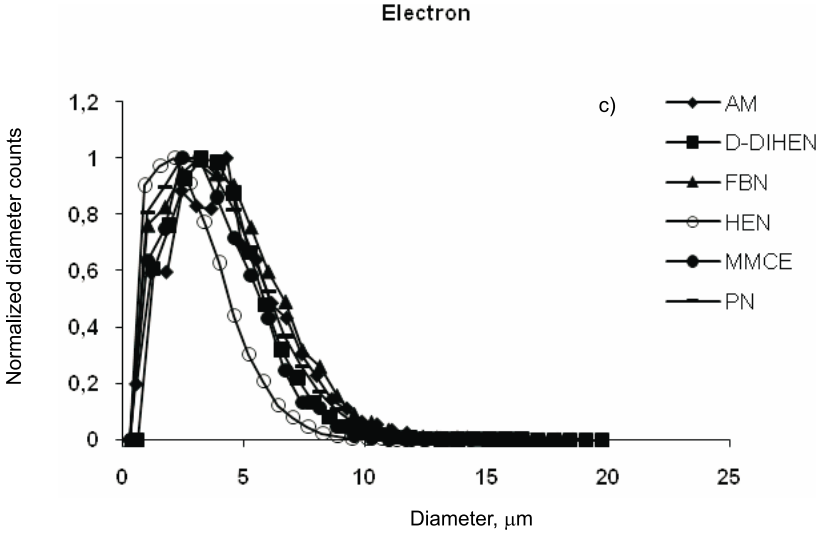

Figure 3. (Continuation)

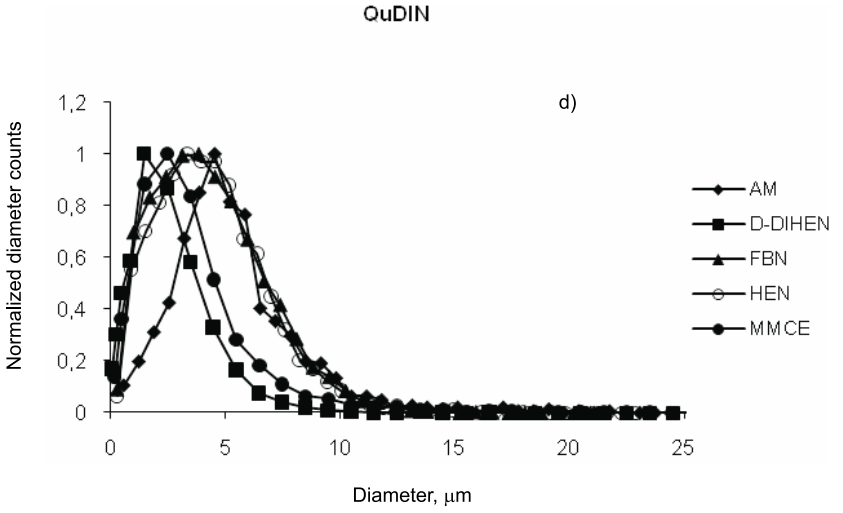

Figure 3. (Continuation)

Drop size and velocity distributions of tertiary aerosols

Figure 3(b)–(d) and 4(b)–(d) show the distributions of drop size and velocity of aqueous tertiary aerosols obtained for all nebulizers and spray chambers studied. The majority of tertiary aerosols in all tested nebulizers appeared in the form of droplets smaller than 20 μm; hence, the single-pass spray chambers and both cyclonic spray chambers showed d_c values of approximately 20 μm and 15 μm, respectively. Droplets larger than 8 μm affected desolvation and vaporization of smaller droplets causing suppression of the emission and ionization processes [12, 29, 30]. The number percentage of tertiary aerosol contained in droplets having sizes smaller than 8 μm was 92%, 98%, 95%, 99%, 98% and 96% for AM, MMCE, FBN, HEN, D–DIHEN and PN when the 'Cinnabar' cyclonic spray chamber was used (Fig. 3(b)). Similar trend was observed for all tested nebulizers connected with the 'Electron', though it can be stated that the filtering action of this spray chamber was slightly higher (Fig. 3(c)). The QuDIN spray chamber required very low sample uptake rates and therefore the measurements performed with this chamber and PN nebulizer were not performed (strong solution accumulation in the chamber). The number percentage of tertiary aerosol contained in droplets having sizes smaller than 8 μm was 89%, 95%, 93%, 93% and 99% for AM, MMCE, FB, HEN and D–DIHEN coupled with the single-pass spray chamber. Finer tertiary aerosols were obtained with cyclonic spray chambers due to the fact that the cut-off diameter of these chambers was smaller than that of QuDIN and larger droplets were more efficiently removed to the wastes. In addition, the finest tertiary aerosols were produced with QuDIN in micronebulizers of the lowest sample uptake rates: D–DIHEN and MMCE (Fig. 3(d)).

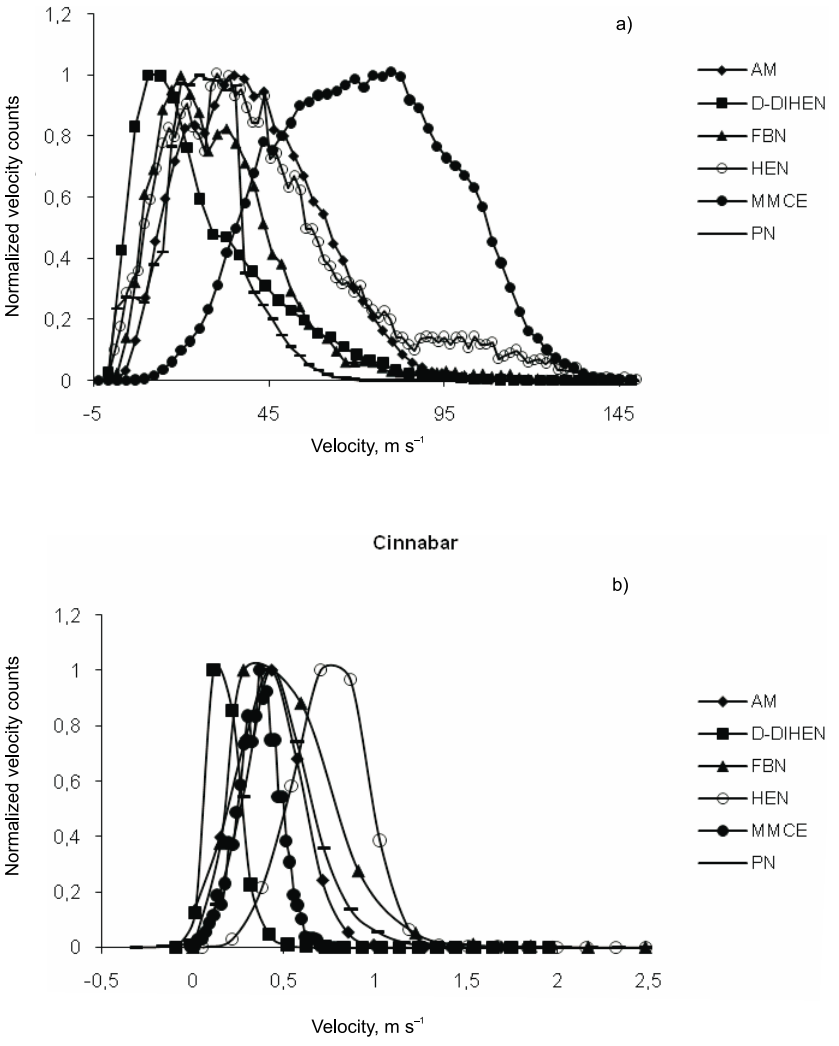

Figure 4. Velocity distributions of primary (a) and tertiary (b)–(d) aerosols from the different nebulizers and spray chambers. (Continuation on the next page)

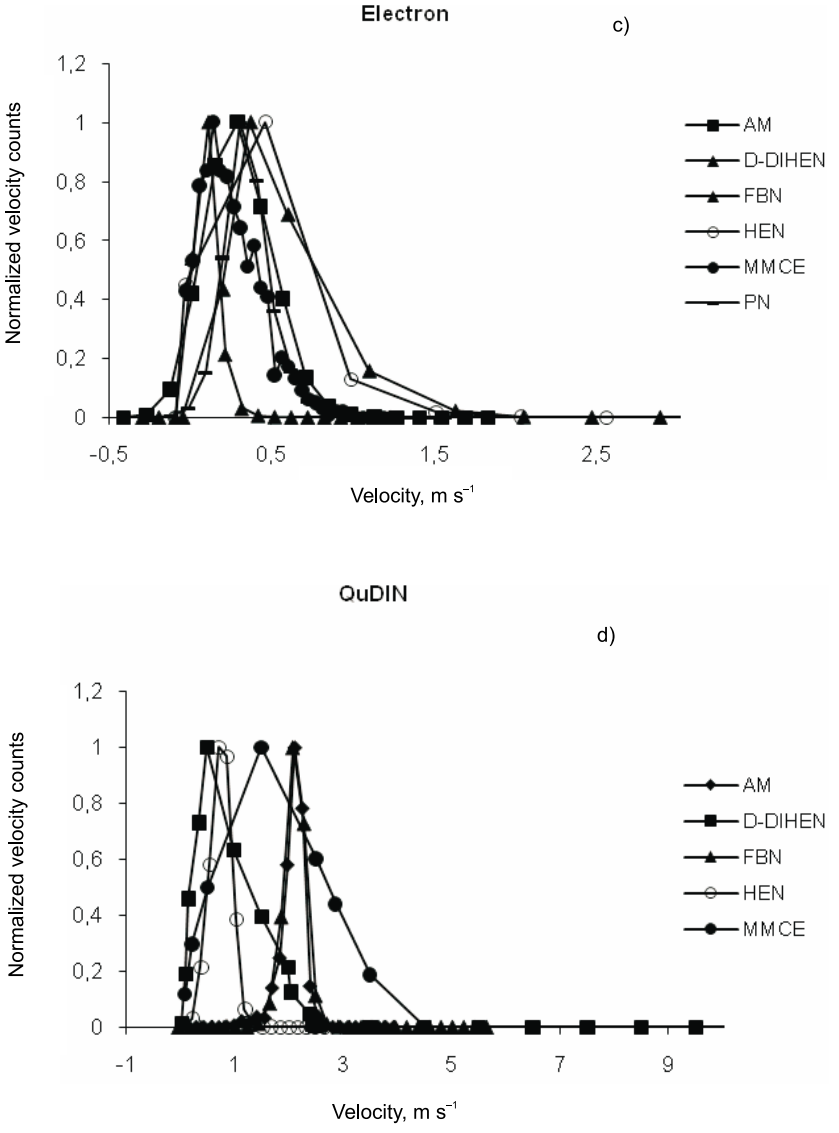

Figure 4. (Continuation)

The shapes of drop size distributions for D–DIHEN, FBN, and HEN primary and tertiary aerosols were similar because the primary aerosol volume was mainly contained in the droplets smaller than the cut-off diameter of the spray chamber used [15]. D–DIHEN, FBN, and HEN generated the finest primary aerosols, whereas both MMCE and PN produced fine tertiary aerosol (slightly better than FBN and comparable to D–DIHEN and HEN). This was the consequence of the spray chamber action

to remove bigger droplets more effectively; filtering action was more intense for MMCE and PN nebulizers.

For all nebulizers coupled with the 'Cinnabar' cyclonic spray chamber the mean velocities of tertiary aerosol were: 0.54, 0.36, 0.49, 0.74, 0.17 and 0.48 m s^{-1} for AM, MMCE, FBN, HEN, D–DIHEN and PN, respectively (Fig. 4(b)). The mean velocities of tertiary aerosol were 0.29, 0.22, 0.38, 0.49, 0.10 and 0.35 m s^{-1} for AM, MMCE, FBN, HEN, D–DIHEN and PN, respectively when the 'Electron' cyclonic spray chamber was used (Fig. 4(c)). The mean velocities of tertiary aerosol produced with QuDIN nebulizer were 2.07, 1.05, 1.69, 0.74 and 0.90 m s^{-1} for AM, MMCE, FB, HEN and D–DIHEN, respectively (Fig. 4(d)). The droplets produced with the single-pass spray chamber were faster than the droplets produced with cyclonic chambers; this was due to the fact that QuDIN had different geometry and required additional gas flow (optimized values were 650 for AM, 500 for both D–DIHEN and MMCE, and 800 mL min^{-1} for FBN and HEN) to prevent solution/aerosol accumulation inside the spray chamber.

Solvent and analyte transport

Both solvent (S_{tot}) and analyte (W_{tot}) transport rates were measured under the optimized conditions of gas and liquid flow rates. S_{tot} and W_{tot} data presented in Table 4 are expressed as the mean values and relative standard deviations of three replicates.

S_{tot} values obtained for all nebulizers tested connected to both 'Cinnabar' and 'Electron' cyclonic spray chambers decreased in the order PN > FBN ≥ HEN >> D–DIHEN > AM >> MMCE. Similar trend was observed for micronebulizers connected to the single-pass spray chamber: FBN ≥ HEN >> D–DIHEN > AM >> MMCE.

W_{tot} values obtained for all nebulizers and spray chambers tested decreased in the order PN > FBN ≥ HEN >> D–DIHEN > AM > MMCE. PN provided the highest solvent and analyte transport. However, it must be taken into account that all micronebulizers worked with significantly lower liquid flow rates than PN. For this reason, the values of solvent (ε_s) and analyte (ε_w) transport efficiencies were calculated (Tab. 5). The obtained ε_s and ε_w values decreased in the order FBN > HEN > D–DIHEN > MMCE > AM > PN. In addition, high solvent transport provided by PN nebulizer could generate plasma cooling because desolvation of an aqueous aerosol required a significant amount of energy. FBN, HEN and D–DIHEN provided high solvent and analyte transport values since they generated the finest primary aerosols and a larger solution mass was allowed to leave the spray chamber.

Table 4. Solvent transport rate ($S_{tot,}$ mg min^{-1}) and analyte transport rate ($W_{tot,}$ µg min^{-1}) for the tested nebulizers and spray chambers

Spray chamber	Nebulizer											
	PN		AM		MMCE		FBN		HEN		D-DIHEN	
	S_{tot}	W_{tot}	S_{tot}	W_{tot}	S_{tot}	W_{tot}	S_{tot}	W_{tot}	S_{tot}	W_{tot}	S_{tot}	W_{tot}
Cinnabar	39.1 ± 4.0	10.2 ± 0.9	2.86 ± 0.21	0.65 ± 0.05	0.64 ± 0.06	0.15 ± 0.01	19.7 ± 1.5	9.55 ± 0.82	18.3 ± 1.5	8.86 ± 0.83	4.01 ± 0.33	1.89 ± 0.16
Electron	38.0 ± 4.2	9.72 ± 0.9	2.93 ± 0.25	0.70 ± 0.06	0.69 ± 0.07	0.16 ± 0.01	18.3 ± 1.4	8.95 ± 0.86	18.4 ± 1.5	8.42 ± 0.80	3.92 ± 0.30	1.96 ± 0.19
QuDIN	–	–	3.52 ± 0.30	0.72 ± 0.06	0.79 ± 0.07	0.20 ± 0.02	17.4 ± 1.4	5.87 ± 0.51	17.7 ± 1.4	5.32 ± 0.49	4.75 ± 0.40	2.19 ± 0.20

Table 5. Solvent transport efficiency (ε_s) and analyte transport efficiency (ε_w) for the tested nebulizers and spray chambers (%)

Spray chamber	Nebulizer											
	PN		AM		MMCE		FBN		HEN		D–DIHEN	
	ε_s	ε_w	ε_s	ε_w	ε_s	ε_w	ε_s	ε_w	ε_s	ε_w	ε_s	ε_w
Cinnabar	2.61 ± 0.25	1.36 ± 0.12	5.72 ± 0.42	2.6 ± 0.20	8.00 ± 0.75	3.75 ± 0.25	23.2 ± 1.7	22.5 ± 1.9	18.3 ± 1.5	17.7 ± 1.7	16.0 ± 1.32	15.1 ± 1.3
Electron	2.53 ± 0.25	1.29 ± 0.12	5.86 ± 0.50	2.8 ± 0.24	8.63 ± 0.88	4.00 ± 0.28	21.5 ± 1.6	21.1 ± 2.0	18.4 ± 1.5	16.8 ± 1.6	15.7 ± 1.20	15.7 ± 1.5
QuDIN	–	–	7.04 ± 0.60	2.9 ± 0.24	9.85 ± 0.88	5.00 ± 0.45	20.5 ± 1.6	13.9 ± 1.2	17.7 ± 1.4	10.6 ± 1.0	19.0 ± 1.60	17.5 ± 1.6

Table 6. The results of MIP–OES analysis of Lobster Hepatopancreas (NRCC TORT–1) certified (standard) reference material (concentrations in μg g^{-1} ± SD of three parallel determinations)

Element	Certified value	PN	AM	MMCE	FBN	HEN	D–DIHEN	NOVA–1
		Found value	Found value	Found value	Found value	Found value	Found value	Found value
Ba	–	–	–	–	–	–	–	–
Ca	0.895 % ± 0.058	0.852 % ± 0.071	0.849 % ± 0.070	0.857 % ± 0.060	0.874 % ± 0.041	0.873 % ± 0.059	0.904 % ± 0.065	0.881 % ± 0.047
Cd	26.3 ± 2.1	27.9 ± 3.5	29.3 ± 4.0	27.2 ± 1.8	26.5 ± 1.4	27.3 ± 2.2	26.8 ± 1.4	27.4 ± 1.9
Cu	439 ± 22	452 ± 41	447 ± 39	447 ± 27	436 ± 31	436 ± 35	431 ± 30	440 ± 27
Fe	186 ± 11	197 ± 22	209 ± 23	176 ± 14	181 ± 15	195 ± 16	192 ± 15	179 ± 11
Mg	0.255% ± 0.025	0.245 % ± 0.023	0.246 % ± 0.018	0.263 % ± 0.015	0.256 % ± 0.010	0.243 % ± 0.017	0.249 % ± 0.014	0.236 % ± 0.013
Mn	23.4 ± 1.0	25.1 ± 2,9	24.8 ± 2.4	24.7 ± 1.5	23.8 ± 1.5	23.9 ± 1.5	24.3 ± 1.5	23.8 ± 1.5
Pb	10.4 ± 2.0	11.5 ± 1.2	10.8 ± 1.0	11.4 ± 0.8	10.6 ± 0.7	11.3 ± 0.9	10.9 ± 0.8	11.2 ±0.9
Sr	113 ± 5	122 ± 12	122 ± 8	117 ± 7	119 ± 5	122 ± 7	120 ± 6	115 ± 6
Zn	177 ± 10	182 ± 21	183 ± 17	183 ± 9	180 ± 12	180 ± 13	172 ±12	181 ±11

Table 7. The results of MIP–OES analysis of Human Hair (NIES CRM–13) certified (standard) reference material (concentrations in μg g^{-1} ± SD of three parallel determinations)

Element	Certified value	PN	AM	MMCE	FBN	HEN	D-DIHEN	NOVA-1
		Found value	Found value	Found value	Found value	Found value	Found value	Found value
Ba	2[a]	< LOD[b]	< LOD[b]	< LOD[b]	2.2 ± 0.2	2.5 ± 0.4	1.8 ± 0.1	2.2 ± 0.3
Ca	820[a]	829 ± 48	826 ± 42	832 ± 50	829 ± 42	832 ± 43	826 ± 42	834 ± 42
Cd	0.23 ± 0.03	< LOD[b]	< LOD[b]	< LOD[b]	< LOD[b]	< LOD[b]	< LOD[b]	< LOD[b]
Cu	15.3 ± 1.2	15.2 ± 1.4	15.7 ± 0.9	15.6 ± 1.0	15.4 ± 1.1	15.7 ± 1.0	15.0 ± 0.9	14.6 ± 0.9
Fe	140[a]	145 ± 17	155 ± 16	149 ± 11	146 ± 12	149 ± 11	151 ± 12	143 ± 9
Mg	160[a]	172 ± 18	170 ± 12	164 ± 12	168 ± 7	172 ± 10	167 ± 9	158 ± 8
Mn	3.9[a]	4.2 ± 0.5	4.4 ± 0.4	4.1 ± 0.3	4.3 ± 0.3	4.3 ± 0.2	4.0 ± 0.2	4.1 ± 0.3
Pb	4.6 ± 0.4	5.0 ± 0.6	5.2 ± 0.6	5.1 ± 0.7	4.4 ± 0.4	4.7 ± 0.6	4.9 ± 0.6	4.4 ± 0.5
Sr	–	–	–	–	–	–	–	–
Zn	172 ± 10	176 ± 16	176 ± 17	179 ± 9	180 ± 11	179 ± 13	175 ± 12	179 ± 11

[a] Non-certified value.
[b] Below limit of detection.

Table 8. The results of MIP–OES analysis of Lichen (IAEA 336) certified (standard) reference material (concentrations in μg g^{-1} ± SD of three parallel determinations)

Element	Certified value	PN	AM	MMCE	FBN	HEN	D-DIHEN	NOVA-1
		Found value	Found value	Found value	Found value	Found value	Found value	Found value
Ba	6.4 ± 1.1	7.9 ± 1.4	7.3 ± 0.9	6.9 ± 0.6	6.7 ± 0.5	6.8 ± 0.6	6.6 ± 0.7	6.2 ± 0.4
Ca	–	–	–	–	–	–	–	–
Cd	0.117[a]	< LOD[b]	< LOD[b]	< LOD[b]	< LOD[b]	< LOD[b]	< LOD[b]	< LOD[b]
Cu	3.6 ± 0.5	4.1 ± 0.5	4.1 ± 0.4	3.5 ± 0.3	3.8 ± 0.3	3.7 ± 0.4	3.4 ± 0.3	3.8 ± 0.3
Fe	430 ± 52	441 ± 53	442 ± 55	435 ± 32	441 ± 35	446 ± 36	439 ± 33	427 ± 27
Mg	–	–	–	–	–	–	–	–
Mn	63 ± 7	68 ± 7	71 ± 6	65 ± 5	68 ± 4	69 ± 5	62 ± 4	66 ± 4
Pb	4.9[a]	4.6 ± 0.5	5.7 ± 0.5	5.5 ± 0.4	5.3 ± 0.4	5.4 ± 0.5	5.2 ± 0.4	5.0 ± 0.4
Sr	9.3 ± 1.1	10.1 ± 1.0	10.2 ± 0.8	9.9 ± 0.7	9.5 ± 0.6	9.4 ± 0.6	9.5 ± 0.5	10.1 ± 0.5
Zn	30.4 ± 3.0	32.9 ± 3.1	33.1 ± 3.9	32.0 ± 2.5	31.8 ± 2.2	31.1 ± 2.2	28.9 ± 2.0	31.4 ± 2.0

[a] Non-certified value.

[b] Below limit of detection.

Table 9. The results of MIP–OES analysis of Soya Bean Flour (INCT SBF–4) certified (standard) reference material (concentrations in μg g^{-1} ± SD of three parallel determinations)

Element	Certified value	PN	AM	MMCE	FBN	HEN	D–DIHEN	NOVA–1
		Found value	Found value	Found value	Found value	Found value	Found value	Found value
Ba	7.30 ± 0.23	7.68 ± 0.75	7.84 ± 0.72	7.72 ± 0.61	7.41 ± 0.30	7.26 ± 0.43	7.49 ± 0.52	7.41 ± 0.48
Ca	2467 ± 170	2489 ± 221	2489 ± 184	2486 ± 137	2516 ± 128	2501 ± 129	2493 ± 125	2475 ± 124
Cd	0.029[a]	< LOD[b]	< LOD[b]	< LOD[b]	< LOD[b]	< LOD[b]	< LOD[b]	< LOD[b]
Cu	14.30 ± 0.46	14.55 ± 1.28	14.70 ± 1.21	14.39 ± 1.01	14.52 ± 1.02	14.52 ± 1.13	14.47 ± 1.01	14.71 ± 0.98
Fe	90.8 ± 4.0	96.4 ± 10.3	94.8 ± 7.6	92.6 ± 7	91.9 ± 7.4	93.7 ± 8	91.4 ± 7	93.6 ± 6
Mg	3005 ± 88	3106 ± 192	3081 ± 193	3054 ± 153	3017 ± 92	3064 ± 146	3022 ± 150	3012 ± 152
Mn	32.3 ± 11	34.3 ± 3.0	37.6 ± 3.5	35.0 ± 2.2	34.1 ± 1.9	34.9 ± 2.8	37.1 ± 2.2	33.9 ± 2.0
Pb	0.083[a]	< LOD[b]	< LOD[b]	< LOD[b]	< LOD[b]	< LOD[b]	< LOD[b]	< LOD[b]
Sr	9.32 ± 0.46	9.62 ± 0.95	9.01 ± 0.74	9.91 ± 0.50	9.50 ± 0.42	9.39 ± 0.52	9.53 ± 0.48	9.47 ± 0.47
Zn	52.3 ± 1.3	58.1 ± 6.8	54.8 ± 5.4	53.1 ± 3.5	54.5 ± 3.3	55.7 ± 4.2	54.2 ± 3.9	54.8 ± 3.4

[a] Non-certified value.

[b] Below limit of detection.

Analysis of reference materials

To evaluate the accuracy and precision of the tested sample introduction systems in the determination of the elements, four certified reference materials (CRMs) were selected for the analysis. The nature of these CRMs was the most similar to that of real biological and environmental samples. The results of the analysis of CRMs by MIP–OES method with nebulization using external calibration are summarized in Tables 6–9. The results of calibration with synthetic aqueous solutions of the analytes agreed with the certified values for all reference materials. Although no interference study was undertaken, it was obvious that there were no matrix-related systematic errors. These results clearly indicated that the employed sample digestion protocol was effective in decomposition of biological and environmental matrices. Precision of replicate determinations was typically around 6% RSD.

CONCLUSIONS

A more efficient atomization principle (*i.e.* Flow Blurring) for liquid sample introduction into MIP–OES instruments has been proposed. A nebulizer based on this new hydrodynamic principle has been favorably compared with five commercial micronebulizers. Detection limits achieved with both FBN and D–DIHEN nebulizers were superior to those obtained with conventional pneumatic nebulizer (PN) and other micronebulizers. In addition, the FB nebulizer was mechanically more robust and could be operated in a broad range of carrier gas rates and sample liquid uptake rates. The analysis of very small samples and particular applications became possible using efficient micronebulizers and MIP–OES technique. All these points allow one to apply the proposed approach to the analysis of samples formerly reserved for GF–AAS only. Practical applications of MIP–OES still give rise to some problems that need to be solved; these difficulties appear however only in case of very complex matrices and slurry sampling analysis, where GF–AAS is still the most attractive alternative. We conclude from this and previous studies [12–15, 17] that the liquid sample introduction system will not be the "Achilles' heel" of atomic spectroscopy any more.

Acknowledgements

Financial support by the Committee of Scientific Research, Poland (Grant No. COST/48/2006) is gratefully acknowledged. BA and AC would like to thank the Spanish Ministry of Education and Science (projects n. PET2006–706–00 and CTQ2005–09079–C03–01/BQU) for the financial support of this work. The authors specially thank the Flow Focusing (USA) and Ingeniatrics S.L. (Spain) for the loan of the Flow Blurring nebulizer. This work was undertaken as part of the EU sponsored COST programme (Action D32, working group D32/005/04, "Microwaves and Ultrasound Activation in Chemical Analysis").

REFERENCES

1. Mora J., Maestre S., Hernandis V. and Todolí J.L., *Trends Anal. Chem*., **22**, 123 (2003).
2. Todolí J.L. and Mermet J.M., *Spectrochim. Acta Part B,* **61**, 239 (2006).
3. Beenakker C.J.M., *Spectrochim. Acta Part B,* **31**, 483 (1976).
4. Stahl R.G. and Timmins K.J., *J. Anal. At. Spectrom.,* **2**, 557 (1987).
5. Jankowski K., Karmasz D. and Starski L., *Spectrochim. Acta Part B*, **52**, 1801 (1997).
6. Yang C., Zhuang Z., Tu Y., Yang P. and Wang X., *Spectrochim. Acta Part B*, **53**, 1427 (1998).
7. Jankowski K., Karmasz D., Ramsza A. and Reszke E., *Spectrochim. Acta Part B*, **52**, 1813 (1997).
8. Matusiewicz H., *J. Anal. At. Spectrom.,* **8**, 961 (1993)
9. Jankowski K., Karaś A., Pysz D., Ramsza A.P. and Sokołowska W., *J. Anal. At. Spectrom.,* **23**, 1290 (2008).
10. Matusiewicz H. and Sturgeon R.E., *Spectrochim. Acta Part B,* **48**, 723 (1993).
11. Matusiewicz H. and Golik B., *Spectrochim. Acta Part B*, **59**, 749 (2004).
12 Almagro B., Ga án-Calvo A.M. and Canals A., *J. Anal. At. Spectrom.,* **19**, 1340 (2004).
13. Almagro B., Ga án-Calvo A.M., Hidalgo M. and Canals A., *J. Anal. At. Spectrom*., **21**, 770 (2006).
14. B Almagro B., Ga án-Calvo A.M., Hidalgo M. and Canals A., *J. Anal. At. Spectrom.*, **21**, 1072 (2006).
15. Matusiewicz H., Ślachciński M., Hidalgo M. and Canals A., *J. Anal. At. Spectrom.*, **22**, 1174 (2007).
16. Ga án-Calvo A.M., *Appl. Phys. Lett*., **86**, 214101/1 (2005).
17. Almagro B., Ga án-Calvo A.M., Hidalgo M. and Canals A., *Evaluation of a new Flow Blurring nebulizer in inductively coupled plasma optical emission spectrometry: Comparative study of several nebulizers and micronebulizers*, (under preparation).
18. Quillfeldt W., *Fresenius' J. Anal. Chem*., **340**, 459 (1991).
19. Matusiewicz H., *Chem. Anal. (Warsaw)*, **40**, 667 (1995).
20. McLean J.A., Zhang H. and Montaser A., *Anal. Chem*., **70**, 1012 (1998).
21. McLean J.A., Huff R.A. and Montaser A., *Appl. Spectrosc,.* **53**, 1331(1999).
22. Smith D.D. and Browner R.F., *Anal. Chem.,* **5**4, 533 (1982).
23. Mora J., Todoli J.L., Rico I. and Canals A., *Analyst,* **123**, 1229 (1998).
24. Matusiewicz H., *Anal. Chem.,* **66**, 751 (1994).
25. Jankowski K. and Jackowska A., *Anal J. At. Spectrom.,* **22**, 1076 (2007).
26. Matusiewicz H. and Golik B., *Microchem. J*., **76**, 23 (2004).
27. Browner R.F., Canals A. and Hernandis V., *Spectrochim. Acta Part B,* **47**, 659 (1992).
28. Todolí J.L., Hernandis V., Canals A. and Mermet J.M., *J. Anal. At. Spectrom*., **14**, 1289 (1999).
29. Hobbs S.E., Olesik J.W., *Anal. Chem.,* **64**, 274 (1992).
30. Olesik J.W., Bates L.C., *Spectrochim. Acta Part B*, **5**0, 285 (1995).

Received May 2009
Revised August 2009
Accepted November 2009